Journal of Solid State Chemistry 184 (2011) 1777–1783

Contents lists available at ScienceDirect

Journal of Solid State Chemistry

journal homepage: www.elsevier.com/locate/jssc

Syntheses and characterization of energetic compounds constructed from alkaline earth metal cations (Sr and Ba) and 1,2-bis(tetrazol-5-yl)ethane

Zhengqiang Xia, Sanping Chen *, Qing Wei *, Chengfang Qiao

Key Laboratory of Synthetic and Natural Functional Molecule Chemistry of Ministry of Education, College of Chemistry and Materials Science, Northwest University, Xi'an, Shaanxi 710069, PR China

ARTICLE INFO

Article history:
Received 4 February 2011
Received in revised form
7 May 2011
Accepted 15 May 2011
Available online 25 May 2011

Keywords:
Coordination polymers
1,2-Bis(tetrazol-5-yl)ethane
Crystal structure
SBUs
Photoluminescence

ABSTRACT

Two new energetic compounds, $[M(BTE)(H_2O)_5]_n$ (M=Sr(1), Ba(2)) [H_2BTE=1,2-bis(tetrazol-5-yl)ethane], have been hydrothermally synthesized and structurally characterized. Single-crystal X-ray diffraction analyses reveal that they are isomorphous and exhibit 2D (4,4) net framework, generated by 4-connected $Sr_2(H_2O)_{10}$/$Ba_2(H_2O)_{10}$ SBUs linked up by two independent binding modes of H_2BTE, and the resulting 2D structure is interconnected by hydrogen-bond and strong face to face π–π stacking interactions between two tetrazole rings to lead to a 3D supramolecular architecture. DSC measurements show that they have significant catalytic effects on thermal decomposition of ammonium perchlorate. Moreover, the photoluminescence properties, thermogravimetric analyses, and flame colors of the as-prepared compounds are also investigated in this paper.

1. Introduction

Tetrazole-based energetic compounds as a class of nitrogen-rich materials with interesting properties have caught the attention of chemists, physicists, and material scientists for their potential application in gas generators [1,2], blowing agents [3–6], primary explosives [7], or ingredients in pyrotechnic and propellant mixtures [8]. They are also very popular in coordination chemistry as ligands through the four nitrogen electron-donating atoms that allow them to serve as either multidentate or bridging building blocks in supramolecular assemblies, medicinal chemistry and various materials science applications as a metabolically stable surrogate for a carboxylic acid group [9,10].

As it is well known, ammonium perchlorate (AP) is one of the most common oxidants in composite solid propellants, and the thermal decomposition characteristics of AP greatly influence the combustion behavior of solid propellants [11,12]. Many effective combustion catalysts on the thermal decomposition of AP, such as metal oxides and other nonenergetic compounds, have been widely reported [13–19]. In order to boost energy levels of propellants, it is anticipated that salts of nitrogen-rich compounds, just like those with 3-nitro-1,2,4-triazol-5-one (NTO), would be used as combustion catalysts to modify the combustion of AP [20,21].

Comparing with traditionary tetrazole ligands, bis(tetrazole) ligands such as *N*,*N*-bis[1(2)H-tetrazol-5-yl]amine, 5,5′-hydrazine-1,2-diylbis(1H-tetrazole), bis(5-tetrazolyl)methane, 1,2-bis(tetrazol-5-yl)ethane, and 1,3-bis(tetrazol-5-yl)propane, not only have high content of nitrogen but also exhibit much more abundant and flexible coordination modes. As a versatile ligand, 1,2-bis(tetrazol-5-yl)ethane (H_2BTE), on one hand, features excellent chemical stability and possesses richer coordination modes owing to the flexible and torsional C–C bond, on the other hand, the tetrazole group acts as the hydrogen-bond acceptor to form hydrogen bonds to construct thermally stable nitrogen-rich compounds. The potential of the 1,2-bis(tetrazol-5-yl)ethane (H_2BTE) to generate nitrogen-rich, highly endothermic metal salts with good performance and high thermal stability has been reported in Tong group's study [22]. Apart from Tong group's study on salts containing the BTE anion, no systematic characterization of its metal salts has been performed to date. In addition, the potential of such compounds for energetic applications (especially in pyrotechnics and propellants) remains to be explored. Considering that alkaline earth metal cations possess variable coordination numbers and special characteristics in flame color, the significance of construct a series of energetic complexes containing alkaline earth metal cations is emerging. Particularly in industrial application, special interest was paid on the investigation of colorant agents for pyrotechnical compositions. However, the energetic complexes of H_2BTE with alkaline earth cations are rarely reported and rules of hard and soft acid–base make the design of corresponding coordination frameworks difficult.

* Corresponding authors. Fax: +86 029 88303798.
E-mail addresses: sanpingchen@126.com (S. Chen), weiqq@126.com (Q. Wei).

0022-4596/$ - see front matter Crown Copyright © 2011 Published by Elsevier Inc. All rights reserved.
doi:10.1016/j.jssc.2011.05.017

In this paper, we synthesized two novel alkaline earth energetic coordination polymers with H_2BTE, $[M(BTE)(H_2O)_5]_n$ (M=Sr(**1**), Ba(**2**)), and investigated the thermostability, flame color, the catalytic performances toward thermal decomposition of AP, and photoluminescent properties. TG-DTG, DSC and flame color experiment revealed that their dehydrated products possess good thermal stabilities up to 350 °C and could be prospectively used as primary ingredients or additives in pyrotechnics and rocket propellants.

2. Experimental section

2.1. Materials and analytical methods

Caution! Tetrazoles are highly energetic compounds with sensitivity toward heat and impact. H_2BTE in its dehydrated form shows increasing friction and impacts sensitivity. Appropriate safety precautions should be taken.

All reagents were purchased commercially and used without further purification. Elemental analyses (C, H, N) were carried out with an Elementar Vario EL III analyzer. IR spectra were recorded with a Tensor 27 spectrometer (Bruker Optics, Ettlingen, Germany). Fluorescent spectra were measured at room temperature with an Edinburgh FL-FS90 TCSPC system. ^{1}H NMR spectra were recorded with a Varian INOVA 400 instrument near 25 °C. Chemical shifts are reported in ppm relative to TMS. The powder X-ray diffraction (PXRD) patterns were measured on a Bruker D8 Advance diffractometer. Thermogravimetric measurements were performed with a Netzsch STA449C apparatus under a nitrogen atmosphere with a heating rate of 10 °C/min from 33 to 800 °C. DSC experiments were performed with a thermal analyzer of Perkin-Elmer Pyris 6 DSC (calibrated by standard pure indium and zinc) with a heating rate of 10 °C/min from 30 to 500 °C.

Table 1
Crystal data and structure refinement summary for compounds **1** and **2**.

Compound	**1**	**2**
Empirical formula	$C_4H_{14}N_8O_5Sr$	$C_4H_{14}N_8O_5Ba$
Formula weight	341.85	391.57
Temperature (K)	296(2)	296(2)
Space group	*Pnnm*	*Pnnm*
a (Å)	11.3352(16)	11.4950(9)
b (Å)	13.8603(19)	14.1859(12)
c (Å)	7.3828(10)	7.6034(6)
α (deg)	90	90
β (deg)	90	90
γ (deg)	90	90
V (Å^3)	1159.9(3)	1239.86(17)
Z	4	4
F(000)	688	760
D_{calcd} (g cm^3)	1.958	2.098
μ (mm^{-1})	4.681	3.234
Data/restraints/parameters	1125/0/115	1196/3/115
GOF on F^2	1.091	1.027
R_1[a] [$I>2\sigma(I)$]	0.0234	0.0200
wR_2[b] (all data)	0.0604	0.0491

[a] $R_1=\sum||F_o|-|F_c||/\sum|F_o|$.
[b] $wR_2=\sum w(F_o^2-F_c^2)^2/\sum w[(F_o^2)^2]^{1/2}$.

2.2. Synthesis

2.2.1. Synthesis of $[Sr(BTE)(H_2O)_5]_n$ (**1**)

A mixture containing $SrCl_2\cdot 2H_2O$ (0.0195 g, 0.1 mmol), H_2BTE (0.0166 g, 0.1 mmol), NaOH (0.0080 g, 0.2 mmol), and H_2O (5 g, 278 mmol) was sealed in a 10-mL Teflon-lined stainless reactor at 110 °C for 3 days. After the sample was cooled to room temperature at a rate of 5 °C/h, the colorless prismatic crystals were collected, washed with water and dried in air. Yield: 56% (based on Sr). Anal. calc. for **1**, $C_4H_{14}N_8O_5Sr$ (M_r=341.85): C 14.05%, H 4.13%, N 32.78%. Found: C 14.02%, H 4.20%, N 32.80%. IR (KBr, cm^{-1}): 3445.6(br, s), 1621.3(m), 1457.1(m), 1399.1(s), 1212.1(m), 1129.6(m), 1071.5(w), 1024.2(w), 790.5(w), 708.8(m), 579.8(s), 462.9(m). ^{1}H NMR (400 MHz, [D$_6$]DMSO): δ=3.443–3.557(br, 10H, H_2O), 2.961-2.970(d, 4H, CH_2CN_4), 2.503–2.511(DMSO) ppm (see Fig. S1).

2.2.2. Synthesis of $[Ba(BTE)(H_2O)_5]_n$ (**2**)

The procedure was the same as that for **1** except that $SrCl_2\cdot 2H_2O$ was replaced by $BaCl_2\cdot 2H_2O$ (0.0244 g, 0.1 mmol), and colorless prismatic crystals were obtained, washed with water and dried in air. Yield: 72% (based on Ba). Anal. calc. for **2**, $C_4H_{14}N_8O_5Ba$ (M_r=391.57): C 12.27%, H 3.60%, N 28.62%. Found: C 12.30%, H 3.71%, N 28.68%. IR (KBr, cm^{-1}): 3437.8(br, s), 1624.3(m), 1463.1(m), 1397.3(s), 1207.6(m), 1132.5(m), 1065.9(w), 1028.1(w), 791.8(w), 706.6(m), 574.2(s), 469.7(m). ^{1}H NMR (400 MHz, [D$_6$]DMSO): δ=3.525(br, s, 10H, H_2O), 2.972–2.980(d, 4H, CH_2CN_4), 2.507(DMSO) ppm (see Fig. S2).

2.3. X-ray crystallography

Diffraction data for **1** and **2** were collected on a Bruker Smart Apex II CCD diffractometer equipped with graphite monochromated Mo$K\alpha$ radiation (λ=0.71073 Å) using ω and φ scan mode at 296(2) K. Absorption correction were applied using the SADABS program [23]. Their structures were solved by direct methods and refined with full-matrix least-squares refinements based on F^2 using SHELXS-97 and SHELXL-97 [24,25]. All non-hydrogen atoms were refined anisotropically. Hydrogen atoms were placed in geometrically calculated positions. Crystallographic data and details on refinements for **1** and **2** are shown in Table 1, selected bond distances and angles are shown in Table S1, and hydrogen bonding interactions for **1** and **2** are shown in Table S2. Further details are provided in the supplementary material.

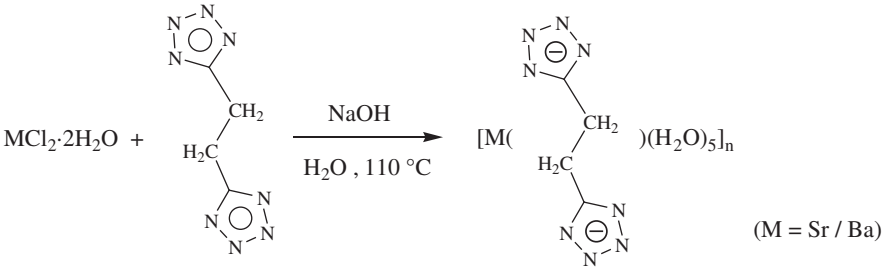

Scheme 1. Strategies for the synthesis of compounds **1** and **2.**

3. Results and discussion

3.1. Syntheses

In the process of synthesis, we attempted to adjust the number of alkyl $(CH_2)_n$ spacers linked bis(tetrazole) ligands through the reactions of the bis(5-tetrazolyl)methane, 1,2-bis(tetrazol-5-yl)ethane, 1,3-bis(tetrazol-5-yl)propane, 1,4-bis(tetrazol-5-yl)butane, and 1,6-bis(tetrazol-5-yl)hexane with alkaline earth metal cations, and anticipated to obtain various crystalline energetic coordination polymers. Unfortunately, we obtained only the title products (Scheme 1), in which the binucleate Sr/Ba clusters act as secondary building units (SBUs) assembled by the multidentate and bridging modes of 1,2-bis(tetrazol-5-yl)ethane. Obviously, the appropriate bond distance and torsion angle of the C–C in H_2BTE played a key role in the construction of the title products. In addition, the hydrothermal method affords a convenient route for preparation of the titled coordination frameworks and obtaining high-quality single crystals suitable for structural determination.

3.2. Structure description

Single-crystal X-ray diffraction studies indicate that **1** and **2** (Fig. S3) are isomorphous, crystallizing in the orthorhombic crystal system, space group *Pnnm*, which features a 2D coordination framework constructed by binuclear Sr/Ba clusters SBUs and BTE ligands. Here, coordination polymer **1** is taken for an example to depict the two-dimensional structure. As shown in Fig. 1, the asymmetric unit of **1** includes two Sr(II) ions, four BTE ligands and ten coordinated water molecules. Each Sr(II) ion center is nine-coordinated by three nitrogen atoms from three BTE ligands (Sr1–N1=2.847(3) Å, Sr1–N2=2.876(3) Å, and Sr1–N8=2.832(3) Å), and six oxygen atoms from six coordinated H_2O molecules (half of which are generated by symmetry) (Sr1–O1=2.5915(17) Å, Sr1–O2=2.588(2) Å, Sr1–O3=2.7321(15) Å, Sr1–O1#1=2.5915(17) Å, Sr1–O2#1=2.588(2) Å, and Sr1–O3#2=2.7321(15) Å), which can be described as a distorted three-capped triangle prism geometry (Fig. 2), where the capping positions are occupied by atom N2, N1, and N8, respectively. And the corresponding bottom quadrilateral faces are formed by O1, O1, O3, O3; O1, O1, O2, O2, and O2, O2, O3, O3, respectively. The Sr(II)–O bond distances range from 2.588(2) to 2.7321(15) Å (Table S1) with the mean of 2.6372(11) Å, which are similar to those observed in other strontium–oxygen complexes with the mean of 2.696(4) Å and 2.636(7) Å [26,27]. Whereas the Sr(II)–N bond distances are slightly longer [2.832(3)–2.876(3) Å], and the N–N bond lengths [1.301(4)–1.351(4) Å] in the tetrazolate rings of **1** are between N–N single bonds (1.454 Å) and N=N double bonds (1.245 Å) [28] (Table S1). This indicates conjugation of the negative charge throughout the aromatic rings as seen in the crystal structures of other compounds containing the BTE anion [29]. In addition, the coordination numbers and distances described above are in agreement with salts with anionic nitrogen heterocycles and compounds with alkaline earth metals [9,30–36].

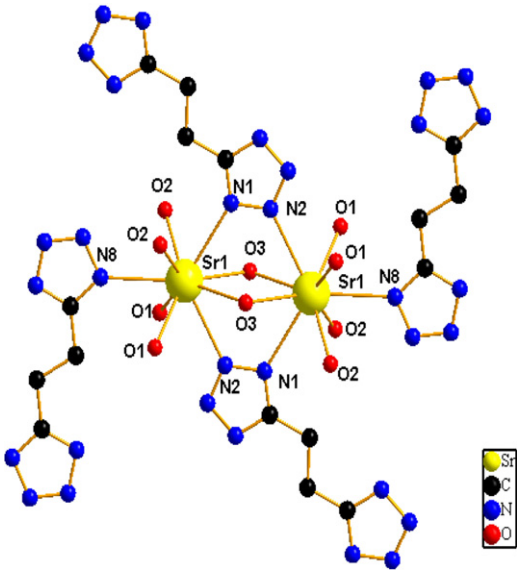

Fig. 1. Coordination environment of Sr(II) ions in **1**, H atoms are omitted for clarity.

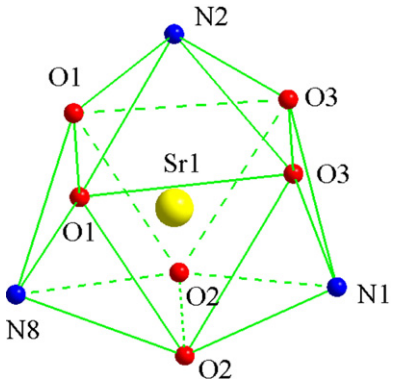

Fig. 2. Coordination polyhedron geometry of Sr(II) in **1**, H atoms are omitted for clarity.

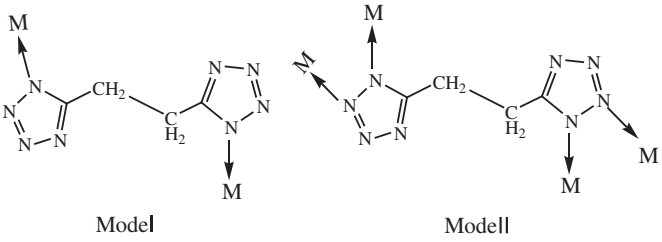

Scheme 2. Coordination modes of H_2BTE in this work.

In the polymeric structure of **1**, the H_2BTE ligand exhibits two distinct types of coordination modes with metal ions (Scheme 2). Notably, two tetrazolate surroundings with the Sr^{2+} are present in this structure: 50% of the tetrazolate rings are coordinated via N1, N2 atoms of BTE through coordination actions along the *a*-axis (Mode II), and 50% of the tetrazolate rings bridge the two Sr^{2+} cations via N8 along the *b*-axis (Mode I) [22,37,38].

In the crystallographically independent unit of **1**, two Sr(II) ions with a distance of Sr…Sr of 4.2889(7) Å are bridged by two coordinated water molecules, forming a binuclear cluster $Sr_2H_{20}O_{10}$, which can be regarded as a SBU (Fig. 3a). These SBUs are connected by BTE ligands in mode II into a one-dimensional zigzag chain along the *a*-axis, and the BTE ligands are further employed in mode I to link the near zigzag chains into a two-dimensional plane along the *c*-axis (Figs. 4 and 3b).

To better understand the structure of **1**, the topological analysis approach is employed, which is a standard procedure for reducing complicated structures to a simple node-and-linker. As discussed above, each building block in **1** is connected to the adjacent four building blocks through tetrazole rings of BTE. Therefore, the dinuclear building blocks are defined as 4-connected nodes, and BTE ligands can act as bridging or multidentate

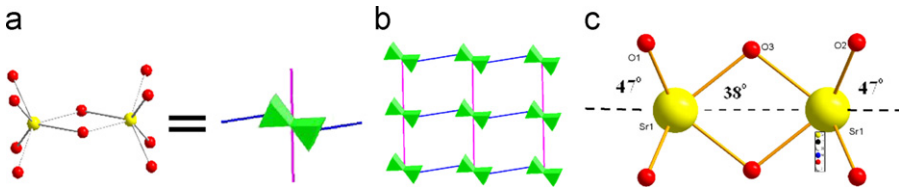

Fig. 3. (a, c) SBU in **1**, the binuclear SBU can be reduced to a green bitripleprism node. The rods in blue and pink represent the two different coordination modes of the ligand. (b) The 2D layer based on the tripleprism node. (All H atoms are omitted for clarity.)

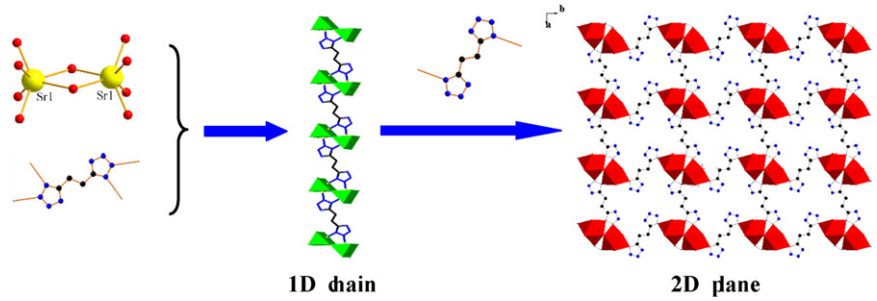

Fig. 4. Polyhedral view of the 1D chain along the *a*-axis and 2D plane along the *c*-axis in **1**. [SrO_6]: green tripleprism; [SrO_6N_3]: red three-capped triangle prism. All H atoms are omitted for clarity.

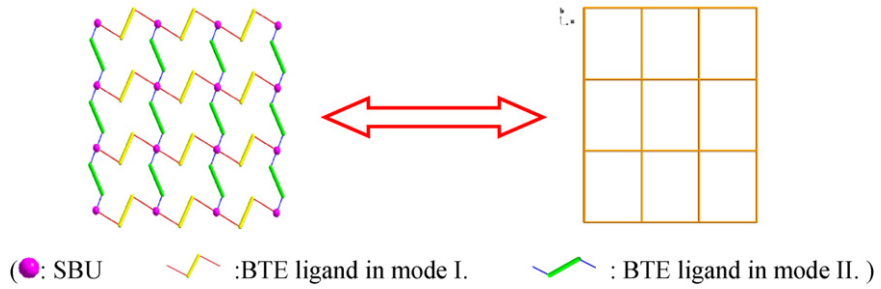

Fig. 5. The simplified 2D structure (left) and the (4,4) topological structure of **1** (right).

ligands that have not been considered in the topological analysis. On the basis of this simplification, the structure of **1** can be described as a four-connected 2D (4,4) network (Fig. 5), in which each lattice has a size of 11.34 × 13.86 Å with the SBUs as knots and BTE ligands as spacers.

It is worth noting that the three kinds of Sr(II)–O bond in a SBU form three angles of 47°, 47°, and 38° to the line of Sr…Sr (Fig. 3c), which give an advantage to generate abundant and strong hydrogen bonds. As shown in Fig. 6, the crystal of **1**, displays tetrazole rings, which is apparently 'coplanar' [39]. The layers of anions are connected with each other by strong, very directional hydrogen bonds to water molecules [O3–H3A···$N6^{(1)}$ 2.991(3) Å; O2–H2WB···$N3^{(2)}$ 2.969(3) Å; O2–H2WA···$N5^{(1)}$ 2.946(3)–Å; O1–H1WA···$N4^{(3)}$ 2.971(3) Å; O1–H1WB···N3 3.364(3) Å and O1–H1WB···N2 3.145(3) Å. Symmetry code: (1) $-x+3/2, y-1/2, -z+1/2$; (2) $x+1/2, -y+3/2, z-1/2$; (3) $x+1/2, -y+3/2, z+1/2$] (Table S2), resulting a 3D supramolecular structure. The water molecules form hydrogen bonds to the ring nitrogen atoms of the BTE anion from the top and from the bottom in five out of the eight ring nitrogen atoms with distances between 2.946(3) and 3.364(3) Å and angles between 121.1° and 176(3)°. Finally, viewing along *b*-axis, an interesting detail in this 3D supramolecular structure is that the Sr(II)–O bonds form the different sizes of diamond-like net (green line in Fig. 6).

Another prominent structural feature of **1** is the existence of the strong intermolecular π–π stacking interactions between the tetrazole rings. The planes of the BTE ligands are parallel with each other, and are stacked such that the distances between planes are close. In **1**, the C1–N5–N6–N7 and C3–N1–N2–N3 tetrazole rings are involved in off-set face-to-face π–π interactions with centroid–centroid separation 3.691 Å (Cg…Cg < 3.7 Å) (Fig. 7), they exhibit strong π–π stacking interactions, which further stabilize the three-dimensional supramolecular framework.

3.3. Thermal analysis and flame color

The typical TG-DTG curves for the crystal samples of **1** and **2** were performed between 33 and 800 °C at a heating rate of 10 °C/min under nitrogen atmosphere. As shown in Fig. S4 for **1**, the TG-DTG curve consists of two-stage mass loss processes, which could be described to that the complex is thermally decomposed into anhydrous Sr(BTE) firstly and further transformed to $SrCO_3$ finally. The first weight loss of 28.58% in the range 100–249 °C corresponds to the expulsion of five coordinated water molecules (calcd. 26.35%), and the latter procedure is completed at 622 °C and the residue corresponds to the predicted $SrCO_3$ (theoretical 43.18%, experimental 41.03%) [40]. In the TG-DTG curve of **2** showed in Fig. S5, **2** remains stable up to 99 °C and then undergoes one-step weight loss of 24.87% from 99 to 143 °C, attributing to the loss of the coordinated water molecules (calcd. 23.00%), the remaining substance shows great stability before 382 °C and then experiences a mass loss of 23.38% (calcd. 26.61%), which stops until 498 °C, corresponding to the generation of the predicted $BaCO_3$. In addition, the end products of **1** and **2** were verified by

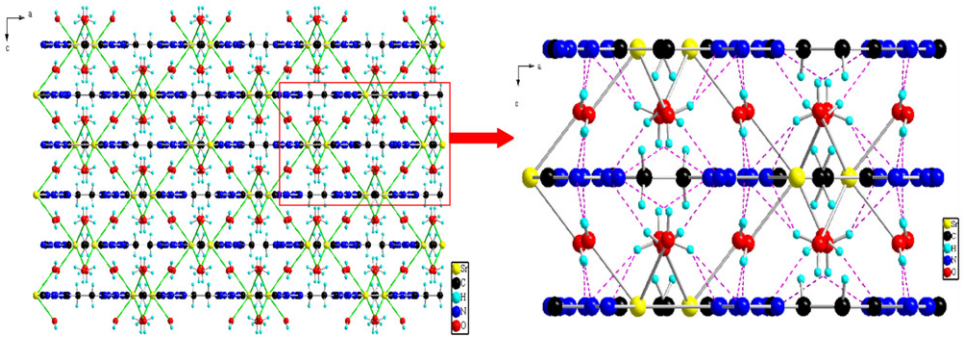

Fig. 6. 3D supramolecular framework assembled via interlayer hydrogen bonds along the *b*-axis in **1**. Where pink dashed lines denote intra-layer hydrogen bonding interactions.

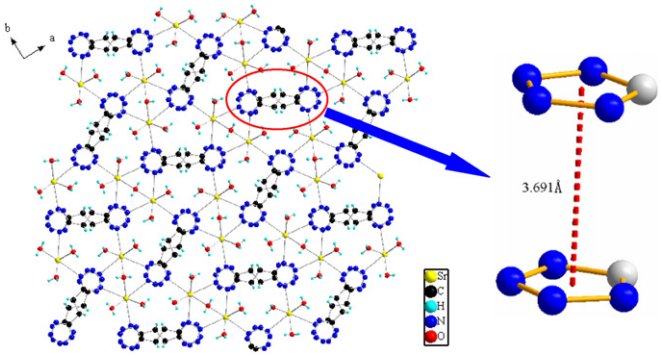

Fig. 7. View of three-dimensional supramolecular architecture of complex **1** in the *ab* plane and π–π stacking interactions of the tetrazole rings in **1** (some H atoms are omitted for clarity).

PXRD experiment (Figs. S6 and S7). Comparing with PXRD patterns of the end product and patterns available in the Powder Diffraction File (JCPDS no. 05-0418 for **1** and 05-0378 for **2**), the results further confirm that the end product of **1** and **2** is just orthorhombic $SrCO_3$ and orthorhombic $BaCO_3$, respectively.

For **1** and **2**, the thermal decomposition profiles are generally quite similar to each other and display mainly two steps of weight losses, which is consistent with their isomorphism substructure skeleton. It is noteworthy that both the frameworks of **1** and **2** exist a high thermal stability (decomposition under N_2 at $T > 350$ °C), which can be attributed to the special 2D plane structures, where they are adopted by 4-connected $Sr_2(H_2O)_{10}$/$Ba_2(H_2O)_{10}$ SBUs linked up by H_2BTE with two independent binding modes, the high coordination number of Sr/Ba, the existence of the hydrogen-bond and the good face to face π–π stacking interactions between tetrazole rings.

In addition, DSC measurements for the two polymers were also investigated by a heating rate of 10 °C/min from 30 to 500 °C. As shown in Fig. 8, both the DSC-data of **1** and **2** show that there exists three consecutive exothermic signals, owing to their isomorphism substructure skeleton. It is remarkable that there are also some significant differences between the complexes, although they have both similar crystal structures. A comparison between **1** and **2** reveals that the thermal stability of **1** is 25 °C lower than that of **2**. In contrast to **2**, the decomposition area of **1** shows two broad exothermic signals, suggesting a complex mechanism of decomposition. In the case of **1**, an endothermic signal at 162 °C indicates the point of dehydration. The shoulder of this signal shows that the dehydration takes place in two steps. However, the points of dehydration of **2** can be clearly distinguished. The first point of dehydration is located at 117 °C, and the second at 130 °C. The difference of the points of dehydration of 45 °C proofs the relatively weaker Ba–O in the barium structure **2**.

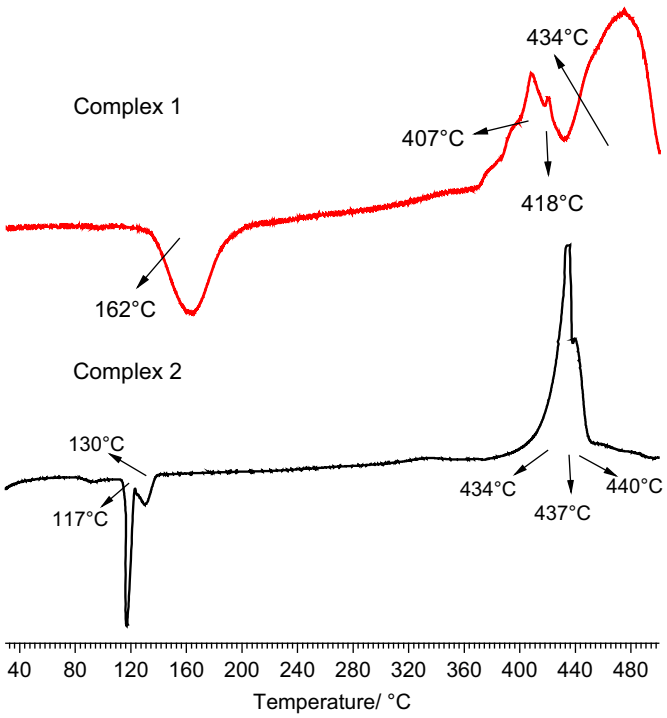

Fig. 8. DSC-plots of compounds **1** and **2**.

This finding is in accordance with the different cation radius in the frameworks.

The flame colors of complexes **1** and **2** are in agreement with the expected colors. **1** decomposes under emission of a slightly red flame color, whereas **2** possesses a pale greenish flame color. For **1** and **2**, the intensity of the flame color is not very high because of the stability of the polymers. The intensity of the color could be achieved by higher temperatures of decomposition, using different oxidizers. These findings cause them to be valuable components for pyrotechnic applications owing to their high energy and high thermal stability.

3.4. Effects on thermal decomposition of ammonium perchlorate [21,41,42]

1/**2** and AP were mixed at a mass ratio of 1:3 to prepare the target samples for thermal decomposition analyses. A total sample mass used was less than 1.0 mg for all runs. From Fig. 9, the endothermic peak at 245 °C for AP is due to a crystallographic transition of AP from orthorhombic to cubic. The second and third peaks for pure AP are exothermic, which is corresponding to the low-temperature decomposition (LTD) process and high-temperature decomposition (HTD)

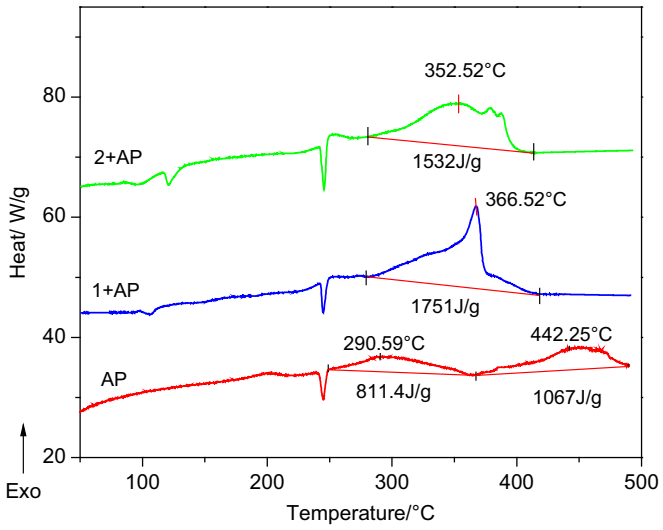

Fig. 9. The integration of DSC curves for AP, **1**+AP, and **2**+AP.

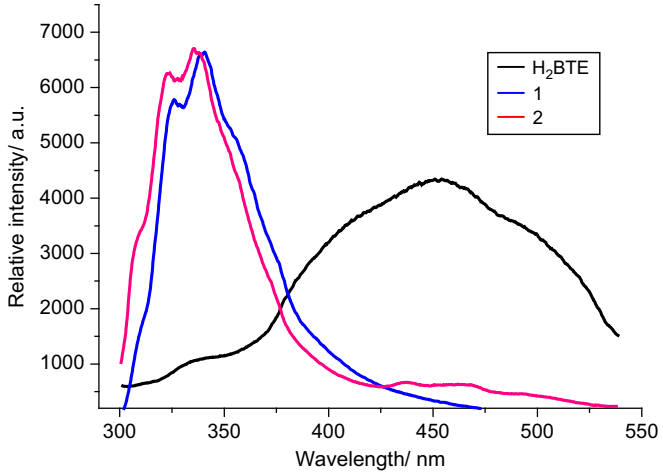

Fig. 10. The emission (λ_{ex}=280 nm) spectra of H_2BTE, **1** and **2** in the solid state at ambient temperature.

process [43,44]. The exothermic peak of the LTD process is at about 290 °C at the heating rate of 10 °C/min, corresponding to the decomposition of AP with the heat of 0.811 kJ/g, while the exothermic peak for HTD process is at 442 °C with the heat of 1.067 kJ/g.

The DSC curves show that the mixture systems of **1**/**2** with AP have no effects on the crystallographic transition temperature, but some significant changes in the decomposition pattern occur. The temperatures of decomposition for the mixture systems, respectively, are much lower than HTD of neat AP. Furthermore, the decomposition heats of the mixture systems are 1.751 and 1.532 kJ/g, respectively, dramatically higher than the corresponding value of neat AP. In the system of **1** with AP, the sharp decomposition peak indicates a rapid process of decomposition, while the second exothermic is absent. The exothermic band of the system of **2** with AP has a series of flat and broad peaks which suggests a complicated mechanism of decomposition, but the max exothermic peak 352.52 °C is lower than HTD of pure AP. Obviously, AP is completely decomposed at the lower temperature in shorter time, which indicates that **1** and **2** are effective catalyst.

3.5. *Luminescence property*

The emission spectra of **1** and **2** in the solid state at room temperature are investigated when irradiated at 280 nm, as shown in Fig. 10. The observation of almost the same emission in complexes **1** and **2**, where BTE has similar conformations with almost the same dihedral angles of the tetrazole rings, which further proves they are isomorphous. **1** shows two strong emission bands with the maximum intensity at 326 and 341 nm, while **2** gives two peaks at 325 and 336 nm. Free H_2BTE exhibits intense blue fluorescent emission bands at 451 nm, attributing to ligand transition π–π^*. It is clear that the large blue-shift of emission occurs in complexes **1** and **2**, which may be due to the π–π^* transition of the ligands and/or the ligand-to-metal charge transfer (LMCT) [37,45–47].

4. Conclusions

In summary, this study provides an example of two novel 2D isomorphous alkaline earth metal complexes based on H_2BTE ligand. Both compounds display (4,4) topologic motif, which is extended through dimeric units connecting with BTE in two different coordination fashions. The thermogravimetric analyses results show these dehydrated coordination polymers exhibit high thermal stability. Furthermore, **1** and **2** in the solid state exhibit strong photoluminescence emission bands and lead to blue-shift, which presumably arises from the π–π^* transition of the ligands and/or the ligand-to-metal charge transfer (LMCT). In addition, the flame color experiments and the effects of them on the thermal decomposition of AP are also explored, which reveal the two polymers not only display expected satisfactory colors but also show good catalytic activity toward decomposition of AP, indicating the potential applications of them for energetic materials as the ingredients or additives in pyrotechnics and propellants.

Supplementary material

CCDC 806955 for **1** and 793811 for **2** contain the supplementary crystallographic data for this paper. These data can be obtained free of charge from The Cambridge Crystallographic Data Centre via www.ccdc.cam.ac.uk/data_request/cif (or from the Cambridge Crystallographic Data Center, 12 Union Road, Cambridge CB2 1EZ, UK; fax: +(44) 1223-336-033; e-mail: deposit@ccdc.cam.ac.uk).

Acknowledgments

We gratefully acknowledge the financial support from the National Natural Science Foundation of China (Grant no. 20873100) and the Nature Science Foundation of Shaanxi Province (Grant nos. FF10091 and SJ08B09).

Appendix A. Supplementary materials

Supplementary materials associated with this article can be found in the online version at doi:10.1016/j.jssc.2011.05.017.

References

[1] R.P. Singh, R.D. Verma, D.T. Meshri, J.M. Shreeve, Angew. Chem. Int. Ed. 45 (2006) 3584.
[2] A.G. Mayants, V.N. Vladimirov, N.M. Razumov, V.A. Shlyapochnikov, J. Org. Chem. 27 (1991) 2177.
[3] Y. Peng, C. Wong, U.S. 5877300, Chung Shan Institute of Science & Technology, March 2, 1999.
[4] M. Kaiser, U. Ticmanis, Inorg. Chem. 40 (2001) 3570.
[5] K. Karaghiosoff, T.M. Klapötke, P. Mayer, C.M. Sabaté, A. Penger, J.M. Welch, Inorg. Chem. 47 (2008) 1007.

[6] T.M. Klapötke, C.M. Sabaté, Heteroat. Chem. 19 (2008) 301.
[7] J. Duguet, Etat Francais, US 4566921, January 28, 1986.
[8] L.V. De Yong, G. Campanella, J. Hazard. Mater. 21 (1989) 125.
[9] M. Friedrich, J.C. Gálvez-Ruiz, T.M. Klapötke, P. Mayer, B. Weber, J.J. Weigand, Inorg. Chem. 44 (2005) 8044.
[10] T.M. Klapötke, G. Steinhauser, Angew. Chem. Int. Ed. 47 (2008) 3330.
[11] L.-J. Chen, L.-P. Li, G.-S. Li, J. Alloys Compd. 464 (2008) 532.
[12] P. Cui, F.-S. Li, J. Zhou, W. Jiang, Propellants Explos. Pyrotech. 31 (2006) 452.
[13] T. Liu, L.-S. Wang, P. Yang, B.-Y. Hu, Mater. Lett. 62 (2008) 4056.
[14] A.A. Said, R. Al-Qasmi, Thermochim. Acta 275 (1996) 83.
[15] X.-F. Sun, X.-Q. Qiu, L.-P. Li, G.-S. Li, Inorg. Chem. 47 (2008) 4146.
[16] D.V. Survase, M. Gupta, S.N. Asthana, Prog. Cryst. Growth Charact. Mater. 45 (2002) 161.
[17] Y.-P. Wang, J.-W. Zhu, X.-J. Yang, L.-D. Lu, X. Wang, Thermochim. Acta 437 (2005) 106.
[18] H. Xu, X.-B. Wang, L.-Z. Zhang, Powder Technol. 185 (2008) 176.
[19] L.-J. Chen, G.-S. Li, L.-P. Li, J. Therm. Anal. Calorim. 91 (2008) 581.
[20] G. Singh, S.P. Felix, Combust. Flame 132 (2003) 422.
[21] P.B. Kulkarni, T.S. Reddy, J.K. Nair, A.N. Nazare, M.B. Talawar, T. Mukundan, S.N. Asthana, J. Hazard. Mater. 123 (2005) 54.
[22] X.-L. Tong, D.-Z. Wang, T.-L. Hu, W.-C. Song, Y. Tao, X.-H. Bu, Cryst. Growth Des. 9 (2009) 2280.
[23] G.M. Sheldrick, SADABS, Software for Empirical Absorption Corrections, University of Gottingen, Germany, 2000.
[24] G.M. Sheldrick, SHELXS-97, Program for Solution of Crystal Structures, University of Gottingen, Germany, 1997.
[25] G.M. Sheldrick, SHELXL-97, Program for Refinement of Crystal Structures, University of Gottingen, Germany, 1997.
[26] R.H. Groeneman, J.L. Atwood, Cryst. Eng. 2 (1999) 241.
[27] H. Ptasiewicz, J. Leciejewicz, J. Coord. Chem. 56 (2003) 223.
[28] A.J. Wilson, International Tables for X-ray Crystallography, vol. C, Kluwer Academic Publishers, Dordrecht, 1992.
[29] A. Hammerl, G. Holl, M. Kaiser, T.M. Klapötke, H. Piotrowski, Z. Anorg. Allg. Chem. 629 (2003) 2117.
[30] A. Hammerl, G. Holl, T.M. Klapötke, P. Mayer, H. Nöth, H. Piotrowski, M. Warchhold, Eur. J. Inorg. Chem. 4 (2002) 834.
[31] I.D. Brown, Acta Crystallogr. B 44 (1988) 545.
[32] J. Hitzbleck, G.B. Deacon, K. Ruhlandt-Senge, Eur. J. Inorg. Chem. 4 (2007) 592.
[33] B. Lian, C.M. Thomas, O.L. Casagrande Jr., T. Roisnel, J.F. Carpentier, Polyhedron 26 (2007) 3817.
[34] T. Zhang, C. Lu, J. Zhang, K. Yu, Propellants Explos. Pyrotech. 28 (2003) 271.
[35] N.C. Mosch-Zanetti, M. Ferbinteanu, J. Magull, Eur. J. Inorg. Chem. 4 (2002) 950.
[36] I. Kobrsi, J.E. Knox, M.J. Heeg, H.B. Schlegel, C.H. Winter, Inorg. Chem. 44 (2005) 4894.
[37] Y.-W. Li, W.-L. Chen, Y.-H. Wang, Y.-G. Li, E.-B. Wang, J. Solid State Chem. 182 (2009) 736.
[38] C. Jiang, Z.-P. Yu, C. Jiao, S.-J. Wang, J.-M. Li, Z.-Y. Wang, Y. Cui, Eur. J. Inorg. Chem. 2004 (2004) 4669.
[39] K. Karaghiosoff, T.M. Klapötke, C.M. Sabaté, Eur. J. Inorg. Chem. 2 (2009) 238.
[40] Q. Shuai, S.-P. Chen, X.-W. Yang, S.-L. Gao, Thermochim. Acta 447 (2006) 45.
[41] M.B. Talawar, C.N. Divekar, P.S. Makashir, S.N. Asthana, J. Propul. Power 21 (2005) 186.
[42] P.W.M. Jacobs, H.M. Whitehead, Chem. Rev. 69 (1969) 551.
[43] S. Vyazovkin, C.A. Wight, Chem. Mater. 11 (1999) 3386.
[44] A.J. Lang, S. Vyazovkin, Combust. Flame 145 (2006) 779.
[45] R.-H. Wang, D.-Q. Yuan, F.-L. Jiang, L. Han, Y.-Q. Gong, M.-C. Hong, Cryst. Growth Des. 6 (2006) 1351.
[46] Y.-C. Chen, K.-B. Wang, Y. Wang, Polyhedron 29 (2010) 669.
[47] W.-T. Liu, Y.-C. Ou, Z.-J. Lin, M.-L. Tong, Cryst. Eng. Commun. 12 (2010) 3487.